A first assessment of organic carbon burial in the West Gironde Mud Patch (Bay of Biscay)

Nicolas Dubosq[a*], Sabine Schmidt[b], J.P. Walsh[c], Antoine Grémare[a], Hervé Gillet[a], Pascal Lebleu[a †], Dominique Poirier[a], Marie-Claire Perello[a], Bastien Lamarque[a], Bruno Deflandre[a]

[a] Univ. Bordeaux, CNRS, EPOC, EPHE, UMR 5805, F-33615 Pessac, France

[b] CNRS, Univ. Bordeaux, EPOC, EPHE, UMR 5805, F-33615 Pessac, France

[c] Coastal Resources Center, University of Rhode Island, Kingstown, RI 02881, USA

*Correspondence to: UMR 5805 EPOC, Université de Bordeaux, Allée Geoffroy Saint-Hilaire, 33615 Pessac CEDEX, France. E-mail address: nicolas.dubosq@u-bordeaux.fr

Abstract

On the Bay of Biscay continental shelf, there are several mid-shelf mud patches including La Grande Vasière to the north, the West Gironde Mud Patch (WGMP) off the Gironde estuary and the Basque Mud Patch close to the Spanish border. In general, these deposits are several meters thick and cover coarser substrate. Questions remain about their storage capability for fine particles and carbon. This work investigates the sedimentation of the WGMP in order to develop a first estimate of organic carbon (OC) burial. Interface sediment cores were collected at nine stations along two cross-shelf transects in October - November 2016. X-radiograph imaging and grain-size analyses were used to characterize sedimentary structures. $^{210}Pb_{xs}$ depth profiles were established to calculate sediment (SAR) and mass (MAR) accumulation rates. Sedimentary structures indicate episodic sandy inputs overlying older deposits at proximal sites, and relatively continuous sedimentation at seaward locations. On the outer-central portion of the northern transect, a maximum SAR (0.47 cm yr^{-1}) was observed, suggesting a depocenter. On the southern transect, excluding two stations where sedimentary inputs appear massive but sporadic, the SARs are lower (<0.3 cm yr^{-1}). Quantitative estimates of OC burial rates increase seaward with a maximum of 45 gC m^{-2} yr^{-1}. To evaluate carbon loading independent of grain-size variability, OC values were normalized to surface area of sediments (SA). Interestingly, a qualitative comparison of OC burial efficiencies using the OC/SA ratio highlights three groups of sites (low, medium and relatively high OC burial efficiency) which are likely related both to different sedimentary environments and variable deposition conditions linked to local environmental conditions and depth. This work highlights the likely control of hydrodynamic intensity and sedimentary inputs on the amount of OC stored in the WGMP sediments.

Keywords: sediment accumulation rate, organic carbon burial, West Gironde Mud Patch, Bay of Biscay, continental shelf

1. Introduction

Organic carbon storage in marine sediments is recognized as a long-term sink for atmospheric carbon dioxide (Berner, 1990, 1982). Understanding the ocean carbon cycle and quantifying carbon storage in the oceans are therefore crucial for improving future climate scenarios (Blair and Aller, 2012; Burdige, 2007; Keil, 2017; Muller-Karger, 2005; Włodarska- Kowalczuk et al., 2019). With about 90% of the modern organic carbon preservation occurring in Rivers-dominated Ocean Margins (RiOMars) systems (Hedges and Keil, 1995; McKee et al., 2004), special attention should be paid to these areas. Although three types of RiOMars have been defined by Blair and Aller (2012), it can be difficult to understand the nature of an individual system because of high spatial and temporal variability (McKee et al., 2004). Owing to these variabilities, each RiOMar can be divided in several sub-environments where major organic carbon (OC) preservation controlling factors may be different (McKee et al., 2004). Moreover, most studies of RiOMars have focused on tropical systems whose results are difficult to translate to higher latitudes (Yao et al., 2014; Zhu et al., 2016). This explains why, in spite of numerous studies on RiOMars (e.g. Aller, 1998; Aller et al., 1996, 1986; Aller and Blair, 2006; Blair and Aller, 2012; Deng et al., 2006; Kuzyk et al., 2017; McKee et al., 2004; Pastor et al., 2018, 2011; Yao et al., 2014; Zhu et al., 2013 and references therein), mechanisms controlling OC preservation in these environments as well as their carbon burial capabilities are not yet fully understood and quantified.

On the Northeast Atlantic margin, the Bay of Biscay continental shelf extends over more than 1000 km, from the Celtic to the North Iberian margins (Borja et al., 2019; Bourillet et al., 2006; Schmidt et al., 2014). Surface shelf sediments are mainly sand. However on the shelf lie also several mid-shelf mud belts and patches including (1) “La Grande Vasière” to the north, (2) the West Gironde Mud Patch off the Gironde estuary and (3) the Basque Mud Patch in front of San Sebastian and Bayonne (**Figure 1**, Allen and Castaing, 1977; Jouanneau et al., 2008, 1999; Lesueur et al., 2002). Overall they are of several meters thick and cover coarser substrate (Jouanneau et al., 1999, 1989; Lesueur et al., 2002, 2001). Mud belts and patches are found on many continental shelves around the world. Typically, they are bounded by dynamic sands on their landward side and are the result of river-derived sediment deposition in areas of lower hydrodynamics (i.e., where waves and currents are more reduced on the seabed; McCave, 1972; Walsh and Nittrouer, 2009). Indeed, their mid-shelf location is directly related to the fact that higher-energy conditions at shallower depth closer to the coast preclude fine sediment accumulation (Dias et al., 2002; McCave, 1972; Walsh and Nittrouer, 2009). These areas are important for biogeochemical transformations and are known organic carbon sinks (McKee et al., 2004).

The West Gironde Mud Patch is particularly interesting because it is under the influence of the Gironde estuary which is the major source of fine sediments for the Bay of Biscay continental shelf (Constantin et al., 2018; Jouanneau et al., 1999, 1989; Lesueur et al., 2002, 1996, 1991; Weber et al., 1991). Studies led in 1990's have rather well defined its sedimentary functioning and suggested a control of sedimentation and resuspension processes by hydrodynamics (Jouanneau et al., 1989; Lesueur et al., 2002, 1991). Only few studies have focused on the WGMP biogeochemistry and ecology (i.e., Massé et al., 2016; Relexans et al., 1992), and have performed too few measurements to characterize its sedimentological, biogeochemical and ecological functioning. This explains why the capability of the WGMP to store OC has not yet been estimated. The present study aims therefore to characterize sedimentation intensity and preferential areas of sediment accumulation in the WGMP to conduct a first estimate of OC burial rates and efficiencies along two cross-shelf bathymetric transects.

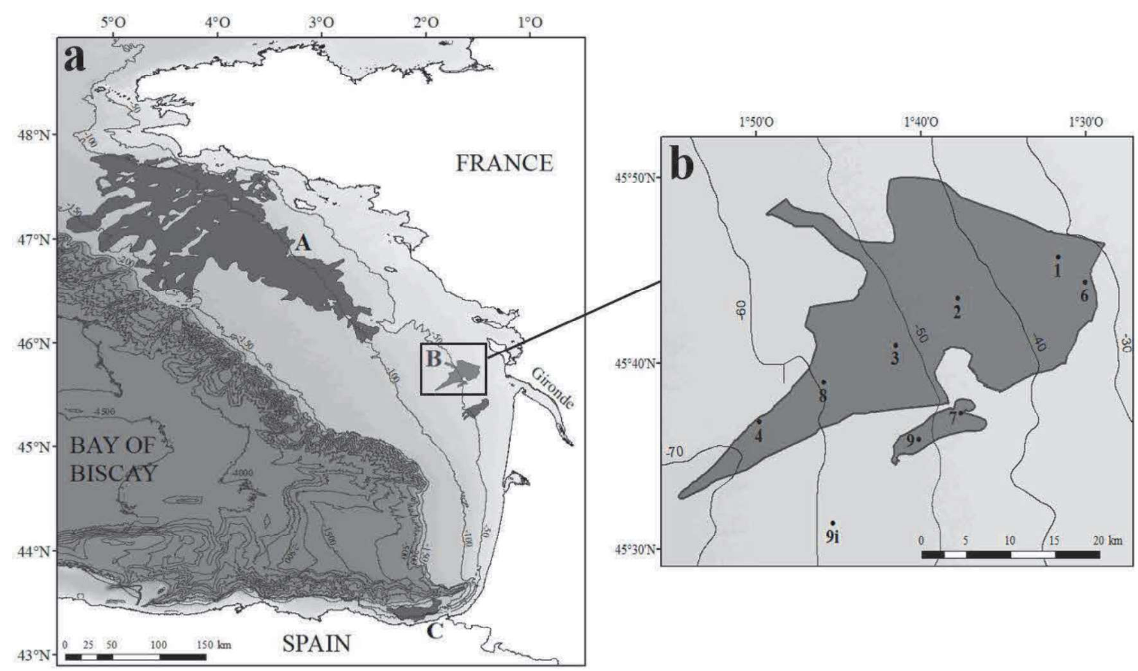

Figure 1: (a) Map of the Bay of Biscay continental shelf with the locations of mud belts and patches: A - La Grande Vasière, B - The Gironde Mud Patches, and C - The Basque Mud Patch. (b) Map of the WGMP showing the location of sampling stations (black circles). The synoptic map of the West Gironde Mud Patch has been determined during the JERICOBENT-5-TH cruise (Gillet and Deflandre, 2018)

2. Material and methods

2.1 Study site

Formed during the Holocene by filling a depression interpreted as a paleo-valley (Lesueur et al., 2002, 1996), the West Gironde Mud Patch is a silty clay sedimentary patch located in the Bay of Biscay, about 15 km seaward of the Gironde estuary mouth (Jouanneau et al., 1989). It lies between 30 and 75 m depth with a surface of about 420 km² (Jouanneau et al., 1989; Lesueur et al., 1991; Massé et al., 2016). The WGMP is influenced by Gironde inputs (Constantin et al., 2018; Jouanneau et al., 1989; Lesueur et al., 2002), which are the highest during river floods (Constantin et al., 2018; Lesueur et al., 2002). On a historical scale, climatic fluctuations (e.g. the "Little Ice Age") and anthropogenic activities like deforestation during the medieval period or estuary management since the XIXth century (e.g. dredging, channel hardening) seem to have modified sediment transport processes and therefore the amount of sediments exported to the shelf (Lesueur et al., 2002, 1996). Sediments are transported from the estuary to the WGMP in a benthic nepheloid layer and believed to be deposited in its deeper part (Weber et al., 1991). During their sedimentation, estuarine particles are mixed with biogenic material (e.g. diatoms) produced in the water column (Weber et al., 1991). In the proximal WGMP, sandy inputs from the adjacent continental shelf can be mixed with silt and clay sediments during storm events (Lesueur et al., 2002; Weber et al., 1991).

2.2 Sampling

The JERICOBENT-1 cruise took place in October - November 2016 on the R/V *Côtes de la Manche* (Deflandre, 2016). Undisturbed sediment cores were collected using a MC6 *Octopus GmbH* multicorer on two transects (**Figure 1**). The northern transect includes five stations (1, 2, 3, 8 and 4), and the southern one has four stations (6, 7, 9 and 9i). At each site, three cores were used to characterize sedimentation. A sediment core (core A) was carefully extruded for radioisotope measurements, every 0.5 cm from the top core to 4 cm and every 1 cm below until the core bottom. A second core (core B) was sliced for organic carbon content and sediment surface area measurements every 0.5 cm over the first centimeter, every 1 cm until 5 cm then every 2 cm until 21 cm and every 5 cm below. All the samples were immediately frozen aboard the ship and kept in the freezer until analysis. An additional sediment core was preserved for X-ray imaging (core C), which was performed within a few days after sampling. Due to the thinness of the mud, station 9i was only sampled for radioisotope measurements before repositioning the vessel.

2.2 Physical characteristics of sediments

Radiographical images which provide a continuous record of sedimentary structures were performed on a longitudinal section of the preserved sediment core using an X-ray imaging system (SCOPIX). Images recorded were converted in 8 bits to bring out sedimentary structures at high resolution (Lofi and Werber, 2001). Dry bulk density (DBD) was calculated on core A by comparing sediment weight before and after drying at 60°C according to the following expression: $DBD = (1-(V_w/(V_w+V_s))*\rho$ with V_w and V_s respectively volumes of water and particles in the sample and ρ, particle density (i.e., 2.65 g cm^{-3}). Sediment grain-size was measured on cores A and B using a Malvern Mastersizer 2000 laser diffraction particle size analyzer. The grain-size distributions being unimodal with the exception of three samples within sandy layers (i.e. cores B, St. 1: 0.5-1 cm, 1-1.5 cm; St. 4: 20-22 cm), median grain-size (D50) and sand content were used as grain-size descriptors.

2.3 Radionuclide analysis

The sedimentation framework was determined based on ^{210}Pb. ^{210}Pb ($T_{1/2}$ = 22.3 years) is a naturally-occurring radionuclide continuously delivered by atmospheric fallout and *in situ* production. This ^{210}Pb, readily scavenged by the particulate phase in the water column and deposited at the seabed by sedimentation, is referred to as ^{210}Pb in excess ($^{210}Pb_{xs}$) of that found within sediment due to the decay of its parent isotope, ^{226}Ra. Radionuclide activities (^{210}Pb, ^{226}Ra) were measured using a high-efficiency, broad energy gamma detector equipped with a Cryo-Cycle II (Mirion). The γ detector is calibrated using IAEA certified materials (RGU-1). Errors on activities are based on standard deviation counting statistics. Excess ^{210}Pb activities were calculated by subtracting the activity supported by its parent, ^{226}Ra, from the total ^{210}Pb activity in the sediment. Sediment layers were measured downcore until reaching negligible $^{210}Pb_{xs}$ activities or the bottom of the core. Sediment and mass accumulation rates (SAR and MAR, respectively) were calculated below the mixed layers from the slope of the $^{210}Pb_{xs}$ profiles against depth and cumulative mass, respectively, using the CF:CS (constant flux and constant sedimentation) model.

It must be noted that ^{137}Cs could be also detected during the same counting sessions. The occurrence of ^{137}Cs ($T_{1/2}$ = 30 years), an artificial radionuclide, is primarily the result of the nuclear weapon test fallout in the early 1960s. In coastal sediments, its detection is an indicator of sediment deposited since 1950. ^{137}Cs activities present low to negligible activities in WGMP sediments, and are not presented in this work. Data (radionuclides, grain-size, dry bulk density) are openly available in a public repository that issues datasets with DOIs (Schmidt, 2020).

2.4 Particulate organic carbon

OC content was measured on freeze-dried pre-weighed sediments using a LECO CS 200. In order to remove carbonates before analysis, an aliquot of about 100 mg was acidified with HCl 2M and dried at 50°C (Cauwet et al., 1990; Etcheber et al., 1999). Sample was then introduced into a furnace where particulate OC combustion produced carbon dioxide which was quantitatively dosed by infrared absorption (Etcheber et al., 1999). The reproducibility of replicated analyses was better than 5%.

Organic carbon contents were normalized to surface area of sediments (SA, expressed in $m^2 g^{-1}$) to minimize variations due strictly to grain-size changes (Hedges and Keil, 1995; Mayer, 1994a). A subsample of freeze-dried sediments was first homogenized and degassed overnight at 150°C. SA was then assessed using a Gemini® VII Surface Area Analyzer (2390a model; Micromeritics®) by a multi-point BET method (Aller and Blair, 2006; Mayer, 1994a).

2.5 Statistical treatment

The significance of correlations between median grain-size and surface area of the sediments and between surface area and organic carbon content was assessed using a Spearman's rank correlation coefficient. These analyses were run with the software SigmaPlot version 14.

3. Results

3.1 Physical characteristics of sediments and sedimentary structures

Sedimentary environments vary in the WGMP. Indeed, although sediments are mainly silt and clay with a median grain-size of 15-20 µm, some peripheral stations (i.e., 1, 6 and 7) have deposits of varying silty and sandy sediments (**Figure 2**). At these sites, median grain-size is higher than 20 µm in some layers of higher sand content (>6%, **Figure 2**). Moreover, the base of these layers is characterized by an erosive contact. The two most proximal stations (i.e., 1 and 6) stand out by having a sandy layer on core top. Based on the grain-size profiles and X-ray images, the thickness of this layer varies from 1 to 4 cm at station 1 depending on cores, which indicates a high spatial variability in the proximal area. Below this surface layer, median grain-size is rather constant with depth but finer than the size measured at other sites, with values around 12 and 10 µm at stations 1 and 6, respectively. Interestingly, similar finer sediments are observed at station 9 from a depth of 17 cm. X-ray images also highlight the presence of thin sandy layers at the shallowest stations (i.e., 1, 2, 3, 6, and 7) which become less frequent with increasing depth (**Figure 2**).

The dry bulk density increases in depth on cores with a rather constant grain-size (e.g. stations 8 and 4, **Figure 2**) as usually observed in interface sediments because of sediment compaction. On the contrary, DBD profiles show variations, usually related to sandy layers, on cores 1, 2, 6, 7 and 9i. These laminae are well preserved in the proximal area (i.e., stations 1 and 6) and at station 7 compared to more distal sites (i.e., 8 and 4) where sediments are homogeneous. The station 9i, at the end of the southern transect is different from the other; it is characterized by a mud deposit of about 14 cm covering a medium sand substratum (**Figure 2**).

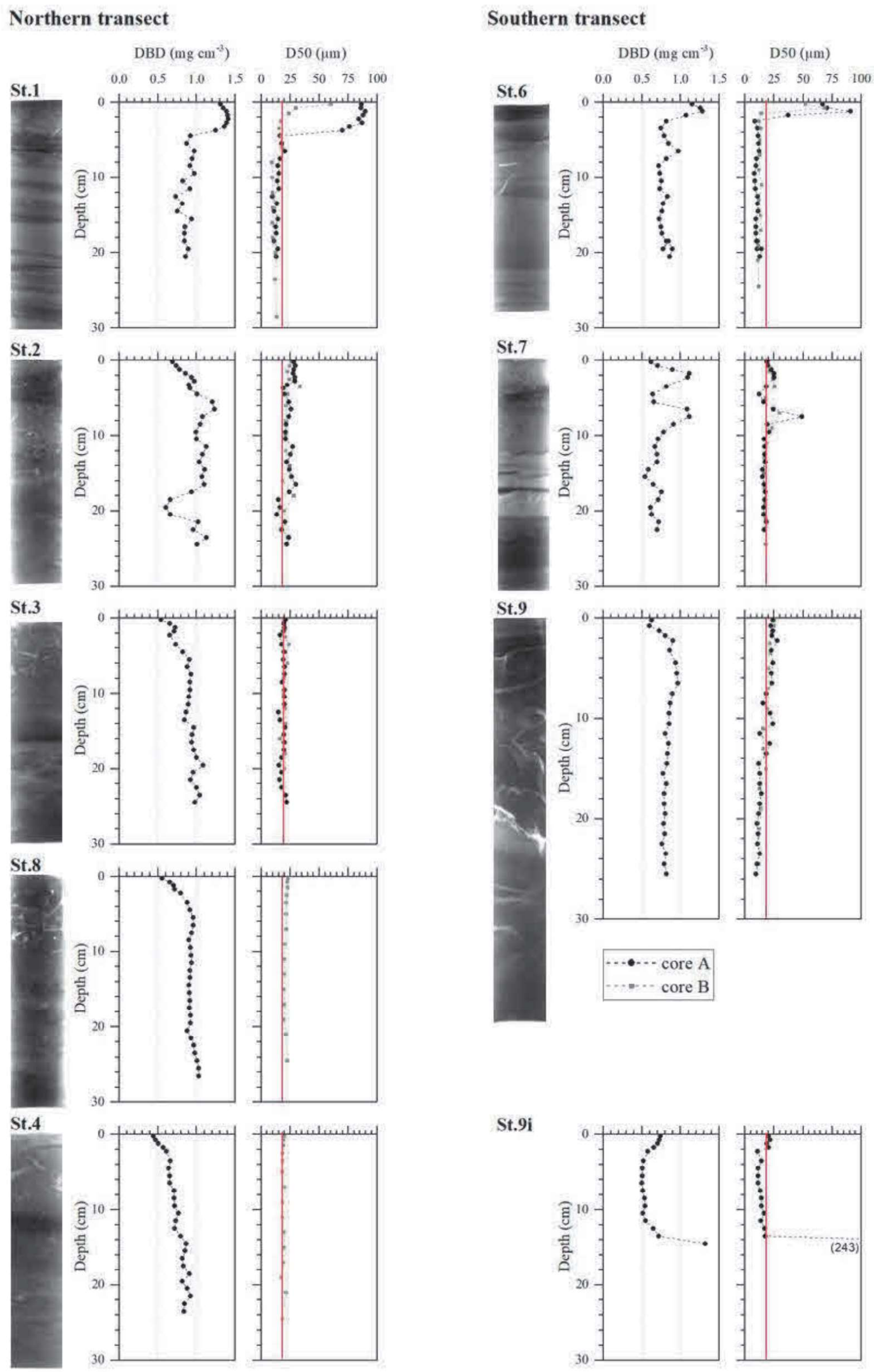

Figure 2: Sedimentary structures: X-ray images and profiles of dry bulk density and median grain-size with depth of cores collecting along the northern (left) and southern (right) transects. The red line defines the background grain-size (~20 µm), and in some cases higher sand content is observed (>6%).

3.2 ^{210}Pb profiles in interface sediments

Along the two depth transects, surface excess ^{210}Pb ranged between 24 and 111 mBq^{-1}, increasing with depth (**Figure 3**). However, the small difference of depth among sites (affecting water column production) cannot account for such low activities at sites 1 and 6. Rather, the lower activities are likely due to dilution by sand. There are three types of $^{210}Pb_{xs}$ profiles. The first group corresponds to the proximal stations 1 and 6. The two most proximal stations present low surface activities, associated with sand, and a rapid activities decrease with depth to reach almost supported levels at about 10-15 cm. These profiles reflect rather low mean apparent sediment and mass accumulation rates, about 0.1-0.2 cm yr^{-1} and < 200 mg cm^{-2} yr^{-1} (**Table 1**). The second group includes stations 7 and 9i along the southern transect, and to a less extent station 2 in the north. The cores present evidence of heterogeneities with depth, as revealed by X-ray images, grain-size and dry bulk density (**Figure 2**, see section 3.1). Such changes in the sediment are likely to impact the $^{210}Pb_{xs}$ activities and are not related to decay. These deep penetration of $^{210}Pb_{xs}$ with depth in the sediment associated with a low activity decrease could reflect massive deposition events. The last group corresponds to cores of the WGMP outer and deepest area, on the north stations 3, 8, and 4 and on the south station 9. At these stations, $^{210}Pb_{xs}$ profiles present a surface mixed layer, followed by a penetration at depths deeper to 25-30 cm. The mixed layer is comprised from 3-4 cm at stations 3 and 8 to 8-9 cm at station 4, indicating an increase of its thickness with depth. Sediment and mass accumulation rates range between 0.29 to 0.47 cm yr^{-1} and 237 to 438 mg cm^{-2} yr^{-1}. Along the northern transect, the highest SARs and MARs are observed at mid-depths (around 50 m). These results are consistent with the outcome of a first investigation of the WGMP sedimentation, based on less vertically-detailed $^{210}Pb_{xs}$ profiles established on cores sampled in 1995 (Lesueur et al., 2001).

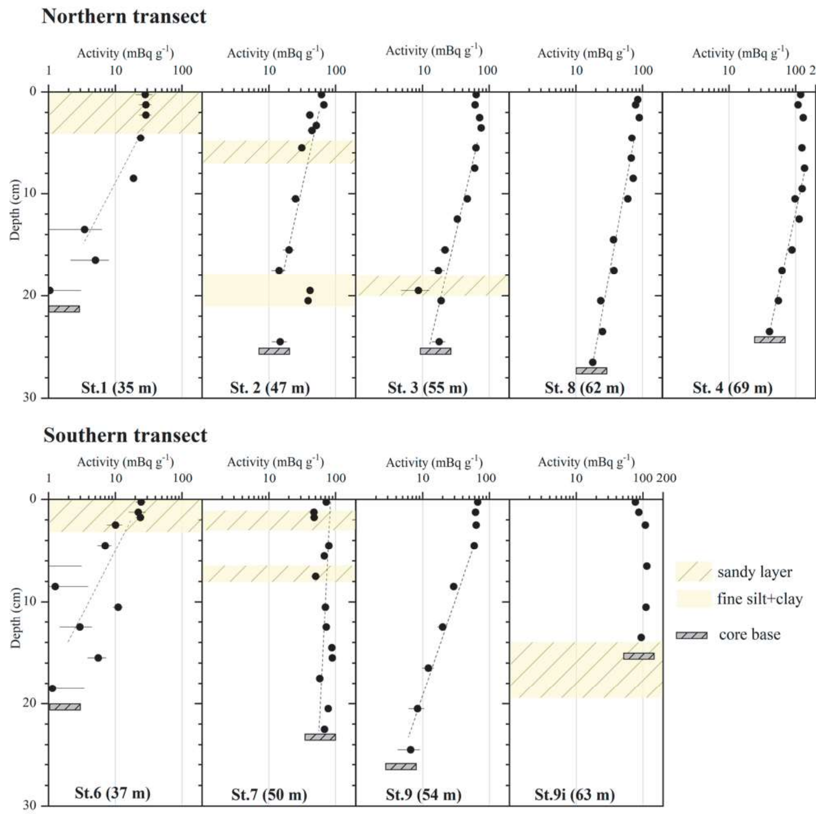

Figure 3: Depth profiles of $^{210}Pb_{xs}$ activity for all the sediment cores collected in the West Gironde Mud Patch in fall 2016. Next to the core label, numbers are the water depth at which the cores were collected. Errors bars correspond to 1 SD. The grey rectangle indicates the length of the core.

Table 1: Mean bottom OC contents, sediment (SAR) and mass (MAR) accumulation rates calculated from $^{210}Pb_{xs}$ profiles and calculated OC burial rates at nine sites of the West Gironde Mud Patch. For stations 1, 6 and 9, the bottom OC values were taken at the base of modern sediments (see Figure 4)

Transect	**Stations**	**Lat.**	**Long.**	**Depth**	**Bottom OC**	***n* =**	**SAR**	**MAR**	**OC burial rates**
		°N	°E	m	%		cm yr^{-1}	mg cm^{-2} yr^{-1}	gC m^{-2} yr^{-1}
North	1	45°45'38"	- 1°31'41"	35	0.64 ± 0.03*	1	0.14 ± 0.08**	126 ± 73**	8 ± 5**
	2	45°43'45"	- 1°37'57"	47	0.66 ± 0.20	5	0.48 ± 0.09**	486 ± 89**	32 ± 16
	3	45°40'58"	- 1°41'30"	55	0.99 ± 0.12	5	0.38 ± 0.04	361 ± 35	36 ± 8
	8	45°38'55"	- 1°45'48"	62	1.02 ± 0.02	5	0.47 ± 0.05	438 ± 47	45 ± 6
	4	45°36'50"	- 1°49'47"	69	1.30 ± 0.04	4	0.41 ± 0.07	338 ± 56	44 ± 9
South	6	45°44'22"	- 1°30'2"	37	0.42 ± 0.27	2	0.22 ± 0.13**	172 ± 102**	7 ± 9**
	7	45°37'17"	- 1°37'34"	50	1.41 ± 0.19	6	0.97 ± 0.20***	648 ± 122***	-
	9	45°35'54"	- 1°40'9"	54	1.17 ± 0.10	3	0.29 ± 0.03	237 ± 22	28 ± 5
	9i	45°31'25"	- 1°45'20"	63	-	-	2.83***	1413***	-

*analytical incertitude
** apparent maximum SAR, MAR and OC burial rates, presence of sandy layers
*** indicative maximum SAR and MAR - not suitable for calculations

3.3 Sedimentary organic carbon

Surface organic carbon contents increase seaward from 0.5 to 1.5% (**Table 2, Figure 4**) as previously reported (Massé et al., 2016; Relexans et al., 1992). Depth OC profiles present different patterns depending on sites as reported for $^{210}Pb_{xs}$. Profiles at stations 3 and 8 present the highest values of OC at the core top which remain rather constant in the mixed layer and then decrease in depth. This pattern is different for stations 1, 2, 6 and 7 which show more erratic profiles where the lowest OC values appear to be associated with sandy layers (**Figure 4**). Mayer (1994a) demonstrated that the relation between OC content and grain-size is related to the adsorption of organic matter on particles, and this can be reinterpreted in terms of the surface area of sediments. Typically, larger-sized particles such as sands have a smaller surface area than smaller-sized particles such as clays. Less organic matter is therefore adsorbed on sandy sediments than on muddy ones. These patterns are observed for the whole WGMP with significant correlations between grain-size and SA (p-value<0.01, **Figure 5a**) and between SA and OC content (p-value<0.01 for the two slopes, **Figure 5c**), indicating that the sediment OC content is at least partly controlled by the grain-size and surface area of particles.

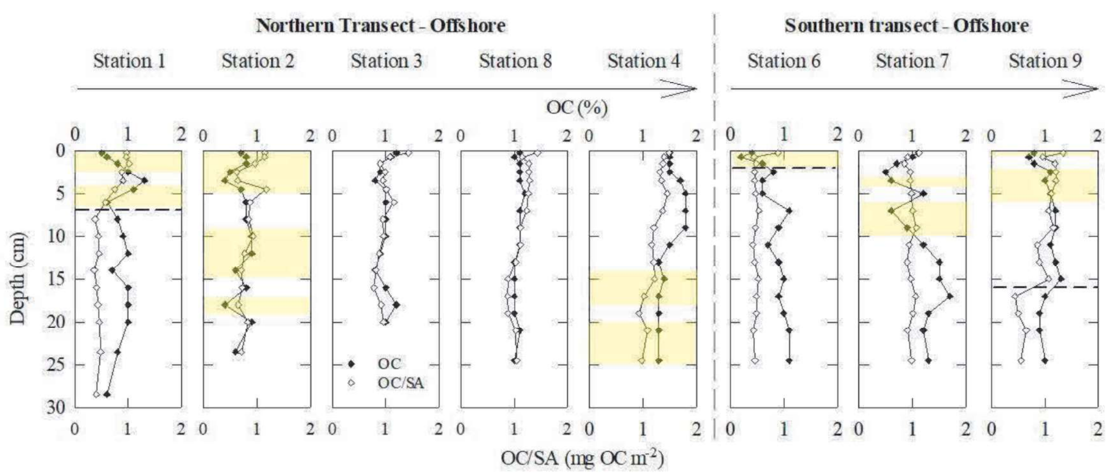

Figure 4: Vertical distributions of OC content (%) and OC/SA ratio (mgOC m^{-2}) in sediment cores collected in the West Gironde Mud Patch. The yellow stripes indicate the position of noticeable sandy layers. Dashed lines represent the limit between modern and relic deposits.

A classical way to minimize OC content variations strictly related to grain-size changes is to normalized OC values to particle SA (Aller and Blair, 2006; Mayer, 1994a, 1994b). An increase of OC/SA ratios in surface sediments is still observed seaward (**Figure 4, Table 2**). The profiles of OC/SA ratio show the highest values on cores top followed by a decrease with depth until reaching a quite constant value at cores bottom. Interestingly, a sharp change of the OC/SA ratio is observed on profiles of stations 1, 6 and 9 under which they are quite constant (**Figure 4**), suggesting the presence of two distinct vertical horizons in the sediment columns. These deposits stand out from most sediments of the WGMP by a lower median grain-size and a higher SA (**Figure 5**). Besides, we observed during slicing that these sediments were visually different, i.e. darker and much stickier. These changes can be related to a variation of sediments in term of sources or ages. From these observations, we interpret the sedimentary columns of cores 1, 6 and 9 as (1) a top part where modern deposition occurs and (2) a bottom part corresponding to old sediments (**Figure 4**). In the rest of the text, the two parts of these cores are respectively qualified as "modern" and "relic" deposits.

Table 2: Surface and bottom core OC contents (%) and OC/SA ratio (mgOC m^{-2}). *For stations 1, 6 and 9 the bottom values were taken at the base of modern sediments.

Stations (Depth)		OC content (%)		OC/SA (mgOC m^{-2})	
		Surface	Bottom	Surface	Bottom
North	1 (35m)	0.48	0.64*	0.97	0.57*
	2 (47m)	0.70	0.56	1.14	0.71
	3 (55m)	1.15	1.02	1.42	0.96
	8 (62m)	1.08	1.01	1.43	1.04
	4 (69m)	1.53	1.25	1.49	0.98
South	6 (37m)	0.36	0.61*	0.89	0.48*
	7 (50m)	1.09	1.32	1.12	0.98
	9 (54m)	0.84	1.25*	1.34	1.07*

The OC/SA ratios at the base of modern sediments vary by more than twice depending on stations and increase with bathymetry with values of 0.5-0.6 mgOC m^{-2} at stations 1 and 6, 0.6-0.9 mgOC m^{-2} at station 2, and about 1.0 mgOC m^{-2} at the other (**Figure 4, Table 2**). Relic sediments at stations 1, 6 and 9 show quite similar OC/SA ratios of 0.42 ± 0.04, 0.47 ± 0.04 and 0.53 ± 0.09 mgOC m^{-2}, respectively (**Figure 4**).

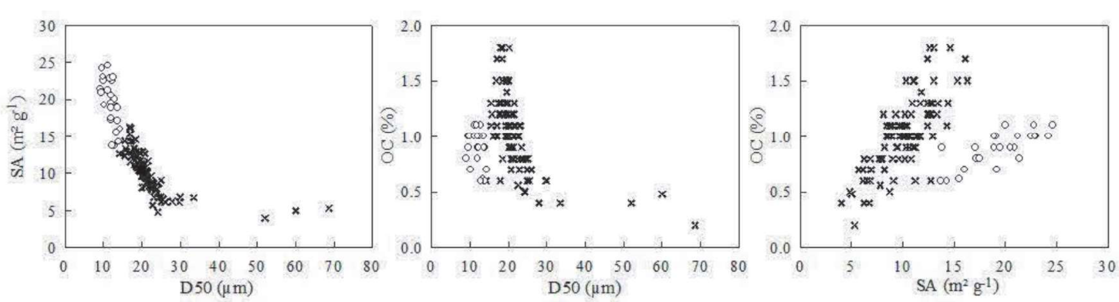

Figure 5: SA against median grain-size (a); Sediment OC content against median grain-size (b) and SA (c). Cross correspond to all the sediment samples, excluding the relic sediments (white circles; stations 1, 6 and 9).

4. Discussion

The sedimentary functioning of the WGMP was first investigated in the late 80s but its capability to store organic carbon on a multi-decennial scale remains still unknown. A prerequisite of establishing estimates of organic carbon burial rates and efficiencies was then to update the present-day sedimentation rates of the area. The potential factors controlling the spatial changes of OC burial rates and storage efficiencies are then discussed, and the capability of the WGMP to store OC is compared to other continental shelfs.

4.1 *Sedimentation in the WGMP*

Sedimentary structures and sedimentation rates in the WGMP suggest a zonation of sedimentary processes in several areas, which differ by hydrodynamic intensity and the constant or transient nature of deposits. The sedimentation appears to be episodic at stations 1, 6, 7 and 9i. In addition, stations 7 and 9i are characterized by massive but sporadic deposits. The sedimentary sequences of interstratified sand and silt layers observed at the most proximal stations 1 and 6 are hypothesized to be the result of alternations of fine particles inputs during river floods and of sand inputs from the adjacent continental shelf during storms (Jouanneau et al., 1989; Lesueur et al., 2002; Weber et al., 1991). The modern sedimentation in the proximal area is related to the surface sandy layers, silty deposits being merely seasonal and resuspended during high hydrodynamic events (Jouanneau et al., 1989; Lesueur et al., 2001), resulting in the lowest SAR reported for the WGMP (**Table 1**). According to literature, relic deposits observed at these sites were dated from 3000 (Jouanneau et al., 1989) to few hundred years B.P. (Lesueur et al., 2002). The deeper and central areas are likely less subjected to hydrodynamic forces (i.e., waves and currents) and thus have higher SAR and MAR (**Figure 6**, **Table 1**). $^{210}Pb_{xs}$ profiles highlight a rather continuous fine sedimentation on the deepest stations of the northern (i.e., 3, 8 and 4) and southern (i.e., 9) transects. SAR of these sites lie a maximum of 0.47 ± 0.05 cm yr^{-1} on the outer-central part of the area, suggesting the presence of a depocenter (**Figure 6**, **Table 1**). The station 2 seems to correspond to a transition area between the proximal and the distal part of the mud patch. It is defined by a rather constant sedimentation interspersed by episodic sandy inputs. Besides the difference in laminae preservation among sites indicates a variation of sediment dynamic. Indeed, the laminae preservation at stations 1, 6 and 7 suggests a high frequency of resuspension/deposition events that prevent to observe biological reworking whereas completely bioturbated facies are observed at distal sites (i.e., 8 and 4). From these results, the WGMP can be divided in three sedimentary areas which can be depicted as: (1) a proximal area subjected to a high hydrodynamics with a low sediment deposition, (2) an outer-central part with a rather constant sedimentation, and (3) patches where deposits seem massive but sporadic.

4.2 Quantitative assessment of OC burial rates in the WGMP

Sedimentation intensity and sediment OC content are known to influence OC storage in sediments (Middelburg, 2019). Therefore, the zonation of sedimentary processes in the WGMP as well as the offshore increase of surface OC content (**Figure 6, Table 2**) suggest that organic carbon burial rates vary depending on areas.

Mean organic carbon burial rates (BR) were determined by multiplying the sediment mass accumulation rate by the mean sediment OC content at the base of modern deposits (Berner, 1982; Masqué et al., 2002; Mayer, 1994a). The non-steady state of sedimentary processes at stations 7 and 9i, precluded the calculation of OC burial rates at these sites. For stations 1 and 6 where the finest fraction is likely to be resuspended during energetic events, burial rates values must be considered as maximum values for the last decades.

On the northern transect, OC burial rates increase seaward from 8 ± 5 gC m^{-2} yr^{-1} at station 1 to almost constant values of about 44 - 45 gC m^{-2} yr^{-1} at depths deeper than 60 m (**Table 2**, **Figure 6**). Indeed, despite the highest sediment OC contents at station 4, OC burial rates are equivalent at stations 4 and 8 owing to a higher MAR at station 8 (**Table 2**, **Figure 6**). This underlines that sediment accumulation intensity is a major controlling factor of organic carbon sequestration on a multi-decennial scale as already reported for other systems like the Rhône delta (Blair and Aller, 2012; Pastor et al., 2011), the Ganges-Brahmaputra Fan (Blair and Aller, 2012), the Eel shelf (Leithold et al., 2005) and more widely for well-oxygenated marine sediments (Blair and Aller, 2012; Canfield, 1994). However, the fact that

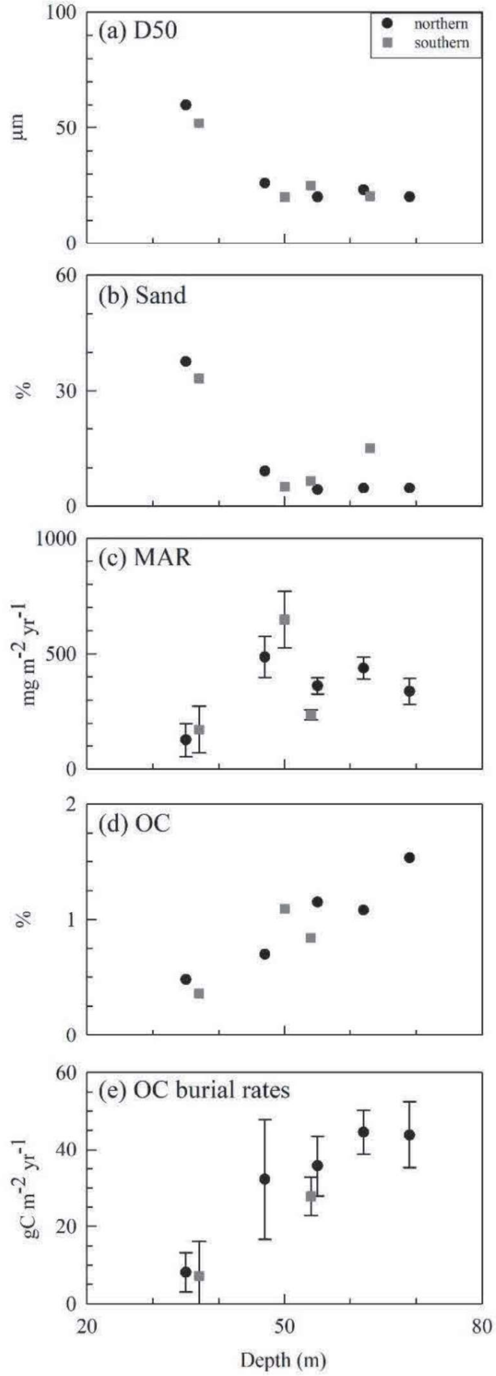

Figure 6: Median grain-size (a), sand (b) and organic carbon (d) content of surface sediments, mass accumulation rates (c) and OC burial rates at multi-decennial scales (e) against water depth of stations along the northern and the southern transects of the West Gironde Mud Patch.

OC burial rates are lower at station 2 in spite of an important MAR indicates that burial rates also depend on OC content. It is indeed lower at this station (**Table 2**) due to the presence of coarser sediments. Organic carbon content at the base of modern deposits is related to (1) organic carbon inputs which are controlled by the type of sedimentation (sand versus mud) and to (2) the extent of organic matter degradation (Middelburg, 2019) whose quantification is out the scope of this work. There are three sediment sources to the WGMP: (1) the Gironde estuary whose particles settle mainly in the central and distal areas, (2) a biogenic production in the water column, and (3) the adjacent continental shelf which supplies sand during energetic events (Jouanneau et al., 1989; Lesueur et al., 2002; Weber et al., 1991). On the northern transect, the decrease of surface median grain-size and sand content seaward indicates a decrease of hydrodynamic intensity with depth (**Figure 6**). This suggests that the type of sedimentation, and so organic matter inputs, are controlled by the hydrodynamic intensity. Sand inputs which occur mainly in the proximal area dilute the sedimentary organic matter whereas higher OC contents are observed in the distal area where hydrodynamic intensity is lower. This clearly shows that the amount of OC stored in the WGMP is influenced by both the amount of sedimentary inputs and hydrodynamic intensity.

4.3 Qualitative comparison of OC burial efficiency: direct use of OC content and SA

The OC burial efficiency is typically assessed with the ratio of OC burial rates to inputs (Burdige, 2007). As these inputs were not quantified in this work, this quantitative approach is ruled out. Nevertheless, the OC/SA ratio allows a qualitative assessment of organic carbon burial efficiencies. Blair and Aller (2012) reported that this ratio can be used to define different types of sedimentary environments (**Figure 7)**. Briefly areas with enhanced organic matter degradation because of frequent sediment remobilization or low sedimentation rates allowing a long oxygen exposure time are characterized by an OC/SA ratio <0.4 mgOC m^{-2}. On the opposite, an OC/SA > 1.0 mgOC m^{-2} reflects an environment with OC inputs higher than loss through degradation (e.g. upwelling or low-oxygen areas). Intermediate values between 0.4 and 1.0 mgOC m^{-2} are observed on river-suspended particles and non-deltaic shelf. In the West Gironde Mud Patch, values of OC/SA ratios at the base of modern sediments are typical of non-deltaic continental shelves (**Table 2**, **Figure 7**), namely those which do not receive high sedimentary inputs (Blair and Aller, 2012; Mayer, 1994a). These values indicate stable organic-mineral associations which protect organic matter from microbial decomposition and result in a lower organic matter reactivity and availability for degradation (Blair and Aller, 2012). This can be due to the supply of relatively refractory organic matter from the Gironde (Etcheber et al., 2007) or to the degradation of organic matter in the sediments of the WGMP until reaching an OC/SA value from which the organic carbon is less bioavailable. The increase seaward of OC/SA ratios at the base of modern sediments indicates an increase of OC storage efficiency (**Table 2**, **Figure 7**). This is consistent with the decrease of hydrodynamic intensity which controls the extent of sediment resuspension. The higher hydrodynamic intensity at proximal sites (i.e., 1 and 6) promotes thus sediment organic matter degradation (Aller, 1998; Aller and Blair, 2006; Yao et al., 2014) and results in a low OC storage efficiency (**Table 2**, **Figure 7**). Conversely, OC storage efficiencies are the highest in the central and distal WGMP. Interestingly, in spite of higher OC burial rates at stations 8 and 4 than at station 3, the three sites seem to be equally efficient to store OC (**Figure 7**). Since the OC contents in surface sediments are higher at station 4, this suggests that organic matter degradation is more efficient at this station than at station 3. The discrepancy between OC burial rates and efficiencies indicates that factors controlling the amount of organic carbon stored in sediments are different than those controlling the preservation efficiency. Therefore, if hydrodynamic intensity and the amount of sedimentary inputs control the quantity of sequestrated OC, the intensity of organic matter degradation may at least in part influence its storage efficiency. Regarding its efficiency to store OC, station 2 can merely be considered as "intermediate". The OC storage at station 7 appears as efficient as at the distal sites (**Figure 7**). This is likely due to the massive sedimentation occurring at this station which limits the degradation of organic matter. However, these deposits may be only transients. Accordingly, it is quite difficult to clearly determine from this study if this storage is efficient on a multi-decennial scale.

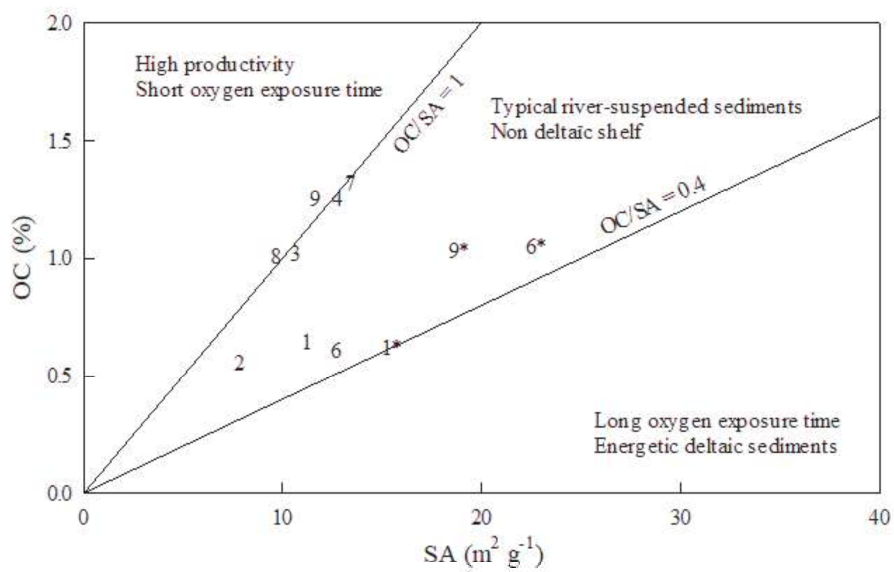

Figure 7: Relationship of OC contents (%) against surface areas of sediments (SA; $m^2\ g^{-1}$) at the base of modern and relic (*) sediments of the West Gironde Mud Patch. Adapted from Blair and Aller (2012).

Relic deposits at stations 1 and 9 present lower OC/SA ratios than modern ones (**Figures 4** and **7**). A first explanation is to consider a longer degradation duration. However, ratios of modern and relic deposits are equivalents at station 6. Low and constant OC/SA ratios (**Figure 4**) indicate that organic matter has been extensively degraded and reached an OC refractory background (Mayer, 1994b, 1994a). This important degradation observed at stations 1 and 6 is likely related to both degradation duration of organic matter and intense hydrodynamics in the inner WGMP.

The use of OC/SA ratios confirms a zonation of sedimentary processes in the WGMP as previously argued on the base of sedimentation characteristics (description, intensity). This could be described in terms of organic carbon storage as: (1) a proximal part characterized by a decimeter-thick modern layer with a relatively low OC storage efficiency overlying relic deposits, (2) a distal area which appears as the only efficient zone for OC storage on a multi-decennial scale, and (3) patches represented by station 7 where apparent efficient OC storage is likely related to massive sedimentation events. These qualitative estimates of OC burial efficiencies confirm that the OC sequestration in the WGMP depends in part on the hydrodynamic intensity which controls sedimentation and resuspension processes. However, other factors like the intensity of organic matter degradation seem influence OC storage efficiency in the central and distal WGMP.

4.4 Comparison with other continental shelves

On the Northeast Atlantic margin, numerous sedimentological and biogeochemical studies have been conducted (Anschutz and Chaillou, 2009; Charbonnier et al., 2019; Herman et al., 2001; Jouanneau et al., 2002; Mouret et al., 2010; Schmidt et al., 2009; van Weering et al., 2002, 1998) but only few of them have focused on the OC sequestration in sediments (Epping et al., 2002; Mouret et al., 2010; van Weering et al., 2002, 1998). Studies conducted on other areas of the Bay of Biscay margin (Mouret et al., 2010) and on the Celtic (van Weering et al., 1998) and Iberian margins (van Weering et al., 2002), allow a comparison with organic carbon burial rates obtained in the WGMP (this work) (**Table 3**). There is a wide range of OC burial rates from <0.5 gC m^{-2} yr^{-1} on the Celtic margin (van Weering et al., 1998) to 34.3 gC m^{-2} yr^{-1} on the Iberian shelf (van Weering et al., 2002). Locally, on the Bay of Biscay margin, organic carbon burial rates decrease with increasing depth, with the highest values observed for the WGMP (**Table 3**). These high OC burial rates are most likely due to the proximity of its main sediment source (i.e., the Gironde). Deeper on the slope, the lower organic carbon burial rates are associated with lower sedimentation rates (**Table 3**, Mouret et al., 2010). Besides, studies carried out on the Iberian shelf and the Celtic margin (i.e., Epping et al., 2002; van Weering et al., 2002, 1998) concluded that, as for the WGMP, variations of OC burial rates are related to variations of sedimentation intensity. These comparisons highlight that the WGMP is an area of the Northeast Atlantic margin which stores relatively high amount of organic carbon on a multi-decennial scale.

At a global oceanic scale, Blair and Aller (2012) reported and compared organic carbon burial efficiencies of many RiOMars. However quantitative estimates of OC burial rates on continental shelves, where fine sedimentation occurs, are mainly related to systems under the influence of large rivers, with average values from 15.3 gC m^{-2} yr^{-1} in the Bohai and Yellow Seas (Hu et al., 2016) to 58.3 gC m^{-2} yr^{-1} in the Amazon deltaic shelf (Aller et al., 1996) (**Table 3**). In addition, the spatial extent of these RiOMars (i.e., at least several thousand square kilometers) makes them important areas for organic carbon storage (Aller et al., 1996; Gordon et al., 2001; Hu et al., 2016; Qiao et al., 2017; Sun et al., 2020). Although the WGMP is one with the highest OC burial rates among the Northeast Atlantic margin systems, it cannot be considered as a major sink of organic carbon on a global oceanic scale due to its small spatial extent (i.e., 420 km²).

Table 3: Mass accumulation rates and OC burial rates in sediments of (1) the West Gironde Mud Patch (this study) (2) the Bay of Biscay (Mouret et al., 2010), (3) the Goban Spur (Celtic margin, Van Weering et al., 1998), (4) the Iberian Margin (Van Weering et al., 2002), (5) the Gulf of Lions shelf (Accornero et al., 2003) and of (6) the Amazon deltaic shelf (Aller et al., 1996; Kuehl et al., 1986), the Bohai and Yellow Seas (Hu et al., 2016), the Zhejiang-Fujian Mud Zone (East China Sea, Sun et al., 2020), the inner Louisiana shelf (Gordon et al., 2001). The most proximal sites of the WGMP (i.e., 1 and 6) are not considered. *Average values of organic carbon burial rates.

Location	Depth (m)	MAR (mg cm^{-2} yr^{-1})	OC burial rates (gC m^{-2} yr^{-1})	References
WGMP (Bay of Biscay)	47 - 69	237 - 486	28 - 45	This study
Bay of Biscay	550	78	7.32	Mouret et al. (2010)
Bay of Biscay	1000	36	2.52	
Bay of Biscay	1250	44	2.4	
Bay of Biscay	1500	7	0.45	
Bay of Biscay	2000	14	0.96	
Goban Spur	208	<5.8	> 0.16	Van Weering et al. (1998)
Iberian Margin	104	204.2	34.30	Van Weering et al. (2002)
Iberian Margin	123	208.9	9.00	
Iberian Margin	199	150.1	7.09	
Iberian Margin	223	157.1	5.02	
Iberian Margin	343	63.4	3.77	
Gulf of Lions	87	230	19.0	Accornero et al. (2003)
Amazon deltaic shelf	9 - 53	100 - 6900	58.3*	Aller et al. (1996), Kuehl et al. (1986)
Bohai and Yellow Seas	0 - 400	< 100 - 7000	15.3*	Hu et al. (2016)
East China Sea	45.4	200 - 700	41.2*	Sun et al. (2020)
Louisiana shelf	4 - 23	120 - 450	22.7*	Gordon et al. (2001)

Conclusion

This study aimed to assess a first estimate of organic carbon sequestration in the West Gironde Mud Patch sediments. The amount of stored OC increases seaward with a maximum value of 45 gC m^{-2} yr^{-1}. Beyond the quantification, sedimentary structures and $^{210}Pb_{xs}$ profiles as well as a qualitative comparison of the capability of each site to store OC allow to divide the WGMP in several sedimentary sub-environments: (1) a proximal area where modern deposits are a decimeter-thick layer with a relatively low OC storage efficiency, (2) a distal part with a relatively efficient OC storage and (3) patches where OC storage seems efficient, at least temporarily.

The amount of OC sequestrated in sediments on a multi-decennial scale is mainly related to the amount of sedimentary inputs and to hydrodynamic conditions which controls sedimentation intensity and nature (i.e., mud versus sand inputs). However other factors like the intensity of organic matter degradation seem to influence the efficiency of OC preservation in sediments in the central and distal areas. Further studies are therefore need to define and quantify processes which can influence this preservation in the West Gironde Mud Patch on a multi-decennial scale but also on other time scales (seasonal, inter-annual, multi-secular). At the scale of the Northeast Atlantic margin, the West Gironde Mud Patch appears efficient in storing organic carbon but its contribution to the OC storage at larger scale remains quite low because of its small surface area. Nevertheless, considering all mud patches of the Bay of Biscay continental shelf (e.g., La Grande Vasière, the Basque Mud Patch), the OC storage can be potentially significant at the North-Atlantic scale. Accordingly, it appears necessary to led further studies on these areas to define their capabilities to store organic carbon.

Acknowledgements

We sincerely acknowledge the captains and crews of the R/V “Côtes de la Manche” (CNRS-INSU) for their great help during the JERICOBENT-1 cruise. We also thank Rémy Synais for his work on sampling and analyses as well as François Dano for the preparation of an updated map of the WGMP during his Master 2 dissertation. This work was supported by: (1) the JERICO-NEXT project (European Union's Horizon 2020 Research and Innovation program under grant agreement no. 654410), (2) the VOG project (national program Interface LEFE-EC2CO). The cruise was funded by the French Oceanographic Fleet (DOI: 10.17600/16010400). A doctoral fellowship was provided to N. Dubosq by the french Ministry of Higher Education, Research and Innovation. We are thankful to the French Nouvelle

Aquitaine Research Council (E3A Project) for co-funding both the low- background gamma detector and the microelectrode system equipped with a camera. We also thank the UMR 5805 EPOC for co-funding the Surface Area Analyzer.

References

Accornero, A., Picon, P., Bovée, F. de, Charrière, B., Buscail, R., 2003. Organic carbon budget at the sediment–water interface on the Gulf of Lions continental margin. Continental Shelf Research 23, 79–92. https://doi.org/10.1016/S0278-4343(02)00168-1

Allen, G.P., Castaing, P., 1977. Carte de répartition des sédiments superficiels sur le plateau continental du Golfe de Gascogne. Bulletin Institut de Géologie du Bassin d'Aquitaine (Bordeaux) 255–261.

Aller, R.C., 1998. Mobile deltaic and continental shelf muds as suboxic, fluidized bed reactors. Marine Chemistry 61, 143–155. https://doi.org/10.1016/S0304-4203(98)00024-3

Aller, R.C., Blair, N.E., 2006. Carbon remineralization in the Amazon–Guianas tropical mobile mudbelt: A sedimentary incinerator. Continental Shelf Research, Special Issue in Honor of Richard W. Sternberg's Contributions to Marine Sedimentology 26, 2241–2259. https://doi.org/10.1016/j.csr.2006.07.016

Aller, R.C., Blair, N.E., Xia, Q., Rude, P.D., 1996. Remineralization rates, recycling, and storage of carbon in Amazon shelf sediments. Continental Shelf Research 16, 753–786. https://doi.org/10.1016/0278-4343(95)00046-1

Aller, R.C., Mackin, J.E., Cox, R.T., 1986. Diagenesis of Fe and S in Amazon inner shelf muds: apparent dominance of Fe reduction and implications for the genesis of ironstones. Continental Shelf Research 6, 263–289. https://doi.org/10.1016/0278-4343(86)90064-6

Anschutz, P., Chaillou, G., 2009. Deposition and fate of reactive Fe, Mn, P, and C in suspended particulate matter in the Bay of Biscay. Continental Shelf Research 29, 1038–1043. https://doi.org/10.1016/j.csr.2008.12.022

Berner, R.A., 1990. Atmospheric Carbon Dioxide Levels Over Phanerozoic Time. Science 249, 1382–1386. https://doi.org/10.1126/science.249.4975.1382

Berner, R.A., 1982. Burial of organic carbon and pyrite sulfur in the modern ocean; its geochemical and environmental significance. American Journal of Science 282, 451–473. https://doi.org/10.2475/ajs.282.4.451

Blair, N.E., Aller, R.C., 2012. The Fate of Terrestrial Organic Carbon in the Marine Environment. Annual Review of Marine Science 4, 401–423. https://doi.org/10.1146/annurev-marine-120709-142717

Borja, A., Amouroux, D., Anschutz, P., Gómez-Gesteira, M., Uyarra, M.C., Valdés, L., 2019. The Bay of Biscay, in: World Seas: An Environmental Evaluation. Elsevier, pp. 113–152. https://doi.org/10.1016/B978-0-12-805068-2.00006-1

Bourillet, J.-F., Zaragosi, S., Mulder, T., 2006. The French Atlantic margin and deep-sea submarine systems. Geo-Marine Letters 26, 311–315. https://doi.org/10.1007/s00367-006-0042-2

Burdige, D.J., 2007. Preservation of Organic Matter in Marine Sediments: Controls, Mechanisms, and an Imbalance in Sediment Organic Carbon Budgets? Chemical Reviews 107, 467–485. https://doi.org/10.1021/cr050347q

Canfield, D.E., 1994. Factors influencing organic carbon preservation in marine sediments. Chemical Geology 114, 315–329. https://doi.org/10.1016/0009-2541(94)90061-2

Cauwet, G., Gadel, F., de Souza Sierra, M.M., Donard, O., Ewald, M., 1990. Contribution of the Rhône River to organic carbon inputs to the northwestern Mediterranean Sea.

Continental Shelf Research 10, 1025–1037. https://doi.org/10.1016/0278-4343(90)90073-U
Charbonnier, C., Mouret, A., Howa, H., Schmidt, S., Gillet, H., Anschutz, P., 2019. Quantification of diagenetic transformation of continental margin sediments at the Holocene time scale. Continental Shelf Research 180, 63–74. https://doi.org/10.1016/j.csr.2019.04.015
Constantin, S., Doxaran, D., Derkacheva, A., Novoa, S., Lavigne, H., 2018. Multi-temporal dynamics of suspended particulate matter in a macro-tidal river Plume (the Gironde) as observed by satellite data. Estuarine, Coastal and Shelf Science 202, 172–184. https://doi.org/10.1016/j.ecss.2018.01.004
Deflandre B., 2016. JERICOBENT-1 cruise, Côtes De La Manche R/V. https://doi.org/10.17600/16010400
Deng, B., Zhang, J., Wu, Y., 2006. Recent sediment accumulation and carbon burial in the East China Sea. Global Biogeochemical Cycles 20. https://doi.org/10.1029/2005GB002559
Dias, J.M.A., Jouanneau, J.M., Gonzalez, R., Araújo, M.F., Drago, T., Garcia, C., Oliveira, A., Rodrigues, A., Vitorino, J., Weber, O., 2002. Present day sedimentary processes on the northern Iberian shelf. Progress in Oceanography, Benthic processes and dynamics at the NW Iberian Margin: results of the OMEX II Program 52, 249–259. https://doi.org/10.1016/S0079-6611(02)00009-5
Epping, E., van der Zee, C., Soetaert, K., Helder, W., 2002. On the oxidation and burial of organic carbon in sediments of the Iberian margin and Nazaré Canyon (NE Atlantic). Progress in Oceanography 52, 399–431. https://doi.org/10.1016/S0079-6611(02)00017-4
Etcheber, H., Relexans, J.-C., Beliard, M., Weber, O., Buscail, R., Heussner, S., 1999. Distribution and quality of sedimentary organic matter on the Aquitanian margin (Bay of Biscay). Deep Sea Research Part II: Topical Studies in Oceanography 46, 2249–2288. https://doi.org/10.1016/S0967-0645(99)00062-4
Etcheber, H., Taillez, A., Abril, G., Garnier, J., Servais, P., Moatar, F., Commarieu, M.-V., 2007. Particulate organic carbon in the estuarine turbidity maxima of the Gironde, Loire and Seine estuaries: origin and lability. Hydrobiologia 588, 245–259. https://doi.org/10.1007/s10750-007-0667-9
Gillet, H., Deflandre, B., 2018. JERICOBENT-5-TH cruise,Thalia R/V. https://doi.org/10.17600/18000425
Gordon, E.S., Goñi, M.A., Roberts, Q.N., Kineke, G.C., Allison, M.A., 2001. Organic matter distribution and accumulation on the inner Louisiana shelf west of the Atchafalaya River. Continental Shelf Research 21, 1691–1721. https://doi.org/10.1016/S0278-4343(01)00021-8
Hedges, J.I., Keil, R.G., 1995. Sedimentary organic matter preservation: an assessment and speculative synthesis. Marine Chemistry 49, 81–115. https://doi.org/10.1016/0304-4203(95)00008-F
Herman, P.M.J., Soetaert, K., Middelburg, J.J., Heip, C., Lohse, L., Epping, E., Helder, W., Antia, A.N., Peinert, R., 2001. The seafloor as the ultimate sediment trap—using sediment properties to constrain benthic–pelagic exchange processes at the Goban Spur. Deep Sea Research Part II: Topical Studies in Oceanography 48, 3245–3264. https://doi.org/10.1016/S0967-0645(01)00039-X
Hu, L., Shi, X., Bai, Y., Qiao, S., Li, L., Yu, Y., Yang, G., Ma, D., Guo, Z., 2016. Recent organic carbon sequestration in the shelf sediments of the Bohai Sea and Yellow Sea, China. Journal of Marine Systems 155, 50–58. https://doi.org/10.1016/j.jmarsys.2015.10.018

Jouanneau, J.-M., Weber, O., Champilou, N., Cirac, P., Muxika, I., Borja, A., Pascual, A., Rodríguez-Lázaro, J., Donard, O., 2008. Recent sedimentary study of the shelf of the Basque country. Journal of Marine Systems, Oceanography of the Bay of Biscay 72, 397–406. https://doi.org/10.1016/j.jmarsys.2007.03.013

Jouanneau, J.M., Weber, O., Cremer, M., Castaing, P., 1999. Fine-grained sediment budget on the continental margin of the Bay of Biscay. Deep Sea Research Part II: Topical Studies in Oceanography 46, 2205–2220. https://doi.org/10.1016/S0967-0645(99)00060-0

Jouanneau, J.M., Weber, O., Drago, T., Rodrigues, A., Oliveira, A., Dias, J.M.A., Garcia, C., Schmidt, S., Reyss, J.L., 2002. Recent sedimentation and sedimentary budgets on the western Iberian shelf. Progress in Oceanography, Benthic processes and dynamics at the NW Iberian Margin: results of the OMEX II Program 52, 261–275. https://doi.org/10.1016/S0079-6611(02)00010-1

Jouanneau, J.M., Weber, O., Latouche, C., Vernet, J.P., Dominik, J., 1989. Erosion, non-deposition and sedimentary processes through a sedimentological and radioisotopic study of surficial deposits from the "Ouest-Gironde vasière" (Bay of Biscay). Continental Shelf Research 9, 325–342. https://doi.org/10.1016/0278-4343(89)90037-X

Keil, R., 2017. Anthropogenic Forcing of Carbonate and Organic Carbon Preservation in Marine Sediments. Annual Review of Marine Science 9, 151–172. https://doi.org/10.1146/annurev-marine-010816-060724

Kuehl, S.A., DeMaster, D.J., Nittrouer, C.A., 1986. Nature of sediment accumulation on the Amazon continental shelf. Continental Shelf Research 6, 209–225. https://doi.org/10.1016/0278-4343(86)90061-0

Kuzyk, Z.Z.A., Gobeil, C., Goñi, M.A., Macdonald, R.W., 2017. Early diagenesis and trace element accumulation in North American Arctic margin sediments. Geochimica et Cosmochimica Acta 203, 175–200. https://doi.org/10.1016/j.gca.2016.12.015

Leithold, E.L., Perkey, D.W., Blair, N.E., Creamer, T.N., 2005. Sedimentation and carbon burial on the northern California continental shelf: the signatures of land-use change. Continental Shelf Research 25, 349–371. https://doi.org/10.1016/j.csr.2004.09.015

Lesueur, P., Jouanneau, J.-M., Boust, D., Tastet, J.-P., Weber, O., 2001. Sedimentation rates and fluxes in the continental shelf mud fields in the Bay of Biscay (France). Continental Shelf Research 21, 1383–1401. https://doi.org/10.1016/S0278-4343(01)00004-8

Lesueur, P., Tastet, J.P., Marambat, L., 1996. Shelf mud fields formation within historical times: examples from offshore the Gironde estuary, France. Continental Shelf Research 16, 1849–1870. https://doi.org/10.1016/0278-4343(96)00013-1

Lesueur, P., Tastet, J.P., Weber, O., 2002. Origin and morphosedimentary evolution of fine-grained modern continental shelf deposits: the Gironde mud fields (Bay of Biscay, France). Sedimentology 49, 1299–1320. https://doi.org/10.1046/j.1365-3091.2002.00498.x

Lesueur, P., Tastet, J.-P., Weber, O., Sinko, J.-A., 1991. Modèle faciologique d'un corps sédimentaire pélitique de plate-forme : la vasière Ouest-Gironde (France). Oceanologica Acta sp., 143–153.

Lofi, J., Werber, O., 2001. SCOPIX - digital processing of X-ray images for the enhancement of sedimentary structures in undisturbed core slabs. Geo-Marine Letters 20, 182–186. https://doi.org/10.1007/s003670000051

Masqué, P., Isla, E., Sanchez-Cabeza, J.A., Palanques, A., Bruach, J.M., Puig, P., Guillén, J., 2002. Sediment accumulation rates and carbon fluxes to bottom sediments at the Western Bransfield Strait (Antarctica). Deep Sea Research Part II: Topical Studies in Oceanography, FRUELA - A Carbon Flux Study in the Antarctic Peninsula Area 49, 921–933. https://doi.org/10.1016/S0967-0645(01)00131-X

Massé, C., Meisterhans, G., Deflandre, B., Bachelet, G., Bourasseau, L., Bichon, S., Ciutat, A., Jude-Lemeilleur, F., Lavesque, N., Raymond, N., Grémare, A., Garabetian, F., 2016. Bacterial and macrofaunal communities in the sediments of the West Gironde Mud Patch, Bay of Biscay (France). Estuarine, Coastal and Shelf Science, Special Issue: Functioning and dysfunctioning of Marine and Brackish Ecosystems 179, 189–200. https://doi.org/10.1016/j.ecss.2016.01.011

Mayer, L.M., 1994a. Surface area control of organic carbon accumulation in continental shelf sediments. Geochimica et Cosmochimica Acta 58, 1271–1284. https://doi.org/10.1016/0016-7037(94)90381-6

Mayer, L.M., 1994b. Relationships between mineral surfaces and organic carbon concentrations in soils and sediments. Chemical Geology 114, 347–363. https://doi.org/10.1016/0009-2541(94)90063-9

McCave, I.N., 1972. Shelf Sediment Transport, Process and Pattern, in: Swift, D.J.P., Duane, D.B., Pilkey, O.H. (Eds.), Transport and Escape of Fine-Grained Sediment from Shelf Areas. Dowden, Hutchinson & Ross, Stroudsburg, Pa., pp. 225–248.

McKee, B.A., Aller, R.C., Allison, M.A., Bianchi, T.S., Kineke, G.C., 2004. Transport and transformation of dissolved and particulate materials on continental margins influenced by major rivers: benthic boundary layer and seabed processes. Continental Shelf Research 24, 899–926. https://doi.org/10.1016/j.csr.2004.02.009

Middelburg, J.J., 2019. Carbon Processing at the Seafloor, in: China's Provincial Economic Competitiveness and Policy Outlook for the 13th Five-Year Plan Period (2016-2020). Springer Singapore, Singapore, pp. 57–75. https://doi.org/10.1007/978-3-030-10822-9_4

Mouret, A., Anschutz, P., Deflandre, B., Chaillou, G., Hyacinthe, C., Deborde, J., Etcheber, H., Jouanneau, J.-M., Grémare, A., Lecroart, P., 2010. Oxygen and organic carbon fluxes in sediments of the Bay of Biscay. Deep Sea Research Part I: Oceanographic Research Papers 57, 528–540. https://doi.org/10.1016/j.dsr.2009.12.009

Muller-Karger, F.E., 2005. The importance of continental margins in the global carbon cycle. Geophysical Research Letters 32, L01602. https://doi.org/10.1029/2004GL021346

Pastor, L., Cathalot, C., Deflandre, B., Viollier, E., Soetaert, K., Meysman, F.J.R., Ulses, C., Metzger, E., Rabouille, C., 2011. Modeling biogeochemical processes in sediments from the Rhône River prodelta area (NW Mediterranean Sea). Biogeosciences 8, 1351–1366. https://doi.org/10.5194/bg-8-1351-2011

Pastor, L., Rabouille, C., Metzger, E., Thibault de Chanvalon, A., Viollier, E., Deflandre, B., 2018. Transient early diagenetic processes in Rhône prodelta sediments revealed in contrasting flood events. Continental Shelf Research 166, 65–76. https://doi.org/10.1016/j.csr.2018.07.005

Qiao, S., Shi, X., Wang, G., Zhou, L., Hu, B., Hu, L., Yang, G., Liu, Y., Yao, Z., Liu, S., 2017. Sediment accumulation and budget in the Bohai Sea, Yellow Sea and East China Sea. Marine Geology 390, 270–281. https://doi.org/10.1016/j.margeo.2017.06.004

Relexans, J.-C., Lin, R.G., Castel, J., Etcheber, H., Laborde, P., 1992. Response of biota to sedimentary organic matter quality of the West Gironde mud patch, Bay of Biscay (France). Oceanologica Acta 15, 639–649.

Schmidt, S., 2020. Depth profiles of selected radionuclides and grain size in marine sediments of the West Gironde Mud Patch (Bay of Biscay). https://doi.org/10.17882/77523

Schmidt, S., Howa, H., Diallo, A., Martín, J., Cremer, M., Duros, P., Fontanier, C., Deflandre, B., Metzger, E., Mulder, T., 2014. Recent sediment transport and deposition in the Cap-Ferret Canyon, South-East margin of Bay of Biscay. Deep Sea Research Part II: Topical Studies in Oceanography 104, 134–144. https://doi.org/10.1016/j.dsr2.2013.06.004

Schmidt, S., Howa, H., Mouret, A., Lombard, F., Anschutz, P., Labeyrie, L., 2009. Particle fluxes and recent sediment accumulation on the Aquitanian margin of Bay of Biscay. Continental Shelf Research, 100 Years of Research within the Bay of Biscay 29, 1044–1052. https://doi.org/10.1016/j.csr.2008.11.018

Sun, X., Fan, D., Liu, M., Liao, H., Tian, Y., 2020. The fate of organic carbon burial in the river-dominated East China Sea: Evidence from sediment geochemical records of the last 70 years. Organic Geochemistry 143, 103999. https://doi.org/10.1016/j.orggeochem.2020.103999

van Weering, T.C.E., de Stigter, H.C., Boer, W., de Haas, H., 2002. Recent sediment transport and accumulation on the NW Iberian margin. Progress in Oceanography, Benthic processes and dynamics at the NW Iberian Margin: results of the OMEX II Program 52, 349–371. https://doi.org/10.1016/S0079-6611(02)00015-0

van Weering, Tj.C.E., Hall, I.R., de Stigter, H.C., McCave, I.N., Thomsen, L., 1998. Recent sediments, sediment accumulation and carbon burial at Goban Spur, N.W. European Continental Margin (47–50°N). Progress in Oceanography 42, 5–35. https://doi.org/10.1016/S0079-6611(98)00026-3

Walsh, J.P., Nittrouer, C.A., 2009. Understanding fine-grained river-sediment dispersal on continental margins. Marine Geology 263, 34–45. https://doi.org/10.1016/j.margeo.2009.03.016

Weber, O., Jouanneau, J.M., Ruch, P., Mirmand, M., 1991. Grain-size relationship between suspended matter originating in the Gironde estuary and shelf mud-patch deposits. Marine Geology 96, 159–165. https://doi.org/10.1016/0025-3227(91)90213-N

Włodarska‐ Kowalczuk, M., Mazurkiewicz, M., Górska, B., Michel, L.N., Jankowska, E., Zaborska, A., 2019. Organic Carbon Origin, Benthic Faunal Consumption, and Burial in Sediments of Northern Atlantic and Arctic Fjords (60–81°N). Journal of Geophysical Research: Biogeosciences 124, 3737–3751. https://doi.org/10.1029/2019JG005140

Yao, P., Zhao, B., Bianchi, T.S., Guo, Z., Zhao, M., Li, D., Pan, H., Wang, J., Zhang, T., Yu, Z., 2014. Remineralization of sedimentary organic carbon in mud deposits of the Changjiang Estuary and adjacent shelf: Implications for carbon preservation and authigenic mineral formation. Continental Shelf Research 91, 1–11. https://doi.org/10.1016/j.csr.2014.08.010

Zhu, C., Wagner, T., Talbot, H.M., Weijers, J.W.H., Pan, J.-M., Pancost, R.D., 2013. Mechanistic controls on diverse fates of terrestrial organic components in the East China Sea. Geochimica et Cosmochimica Acta 117, 129–143. https://doi.org/10.1016/j.gca.2013.04.015

Zhu, M.-X., Chen, K.-K., Yang, G.-P., Fan, D.-J., Li, T., 2016. Sulfur and iron diagenesis in temperate unsteady sediments of the East China Sea inner shelf and a comparison with tropical mobile mud belts (MMBs): S and Fe Diagenesis in Sediments. Journal of Geophysical Research: Biogeosciences 121, 2811–2828. https://doi.org/10.1002/2016JG003391

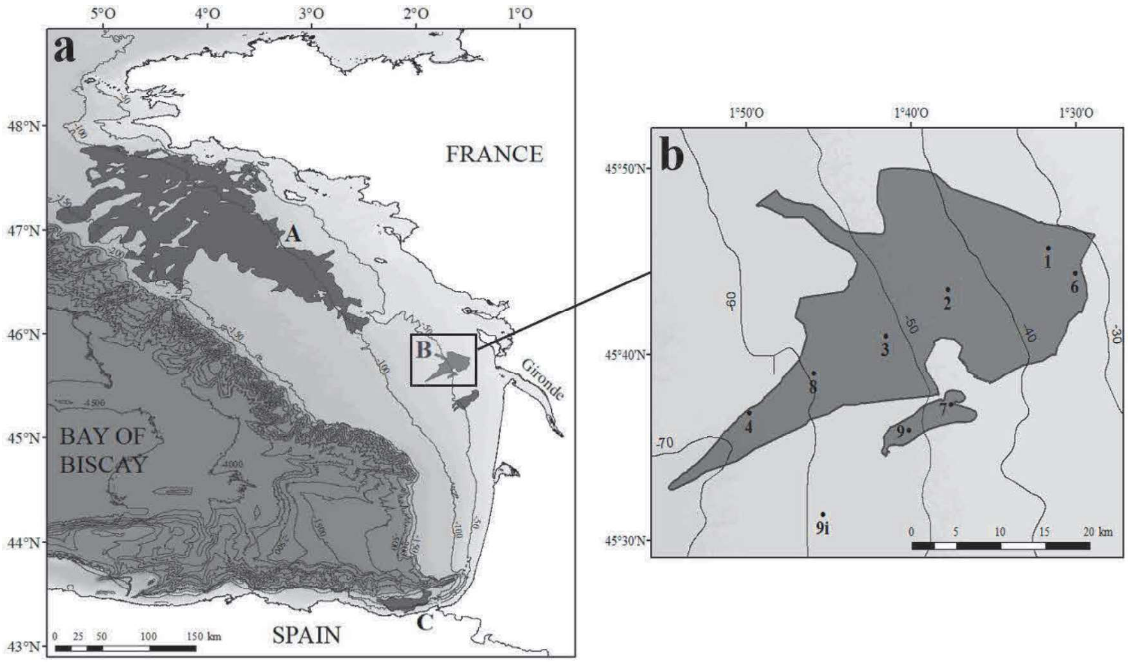

Figure 1: (a) Map of the Bay of Biscay continental shelf with the locations of mud belts and patches: A - La Grande Vasière, B - The Gironde Mud Patches, and C - The Basque Mud Patch. (b) Map of the WGMP showing the location of sampling stations (black circles). The synoptic map of the West Gironde Mud Patch has been determined during the JERICOBENT-5-TH cruise (Gillet and Deflandre, 2018)

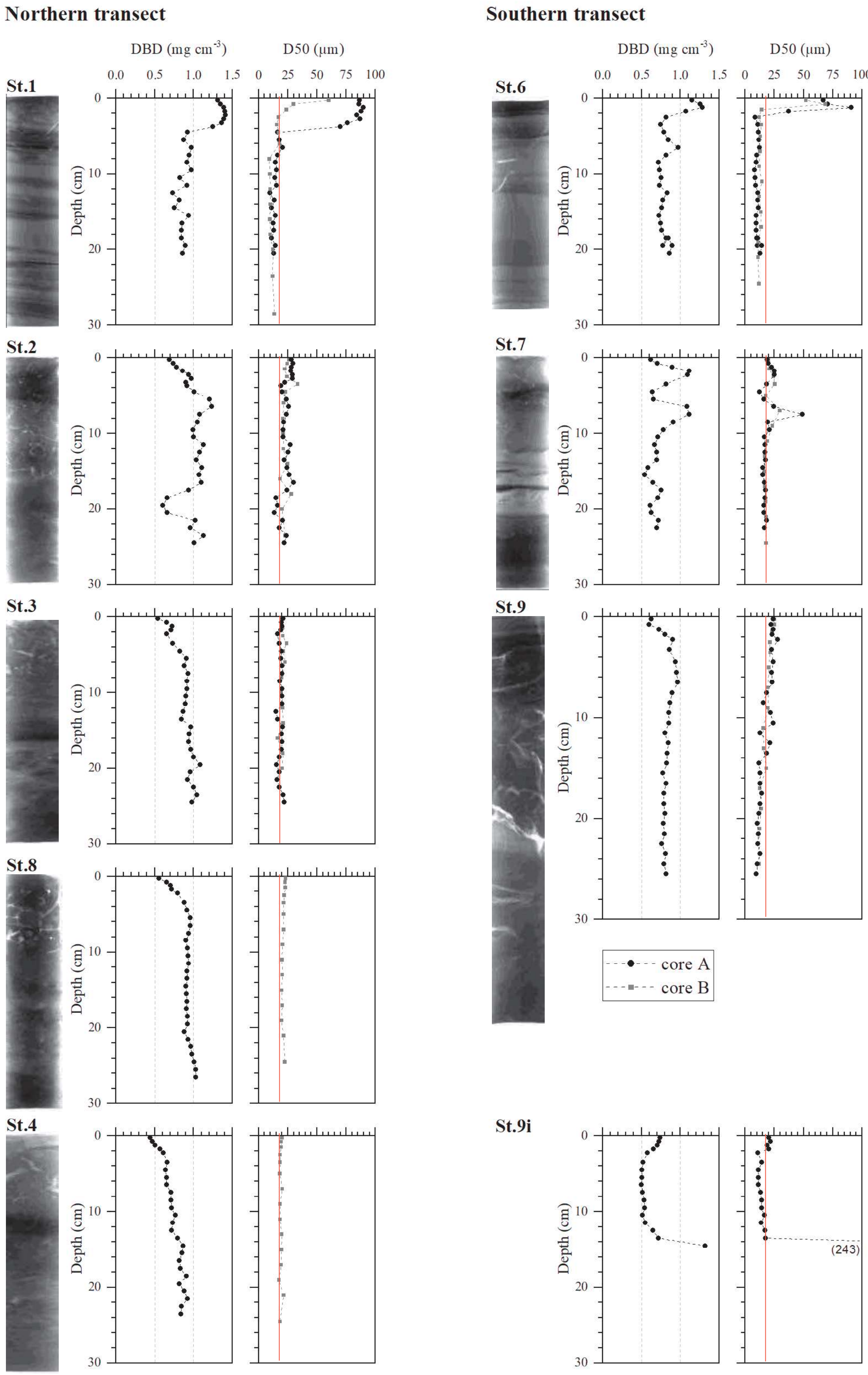

Figure 2: Sedimentary structures: X-ray images and profiles of dry bulk density and median grain-size with depth of cores collecting along the northern (left) and southern (right) transects. The red line defines the background grain-size (~20 μm), and in some cases higher sand content is observed (>6%).

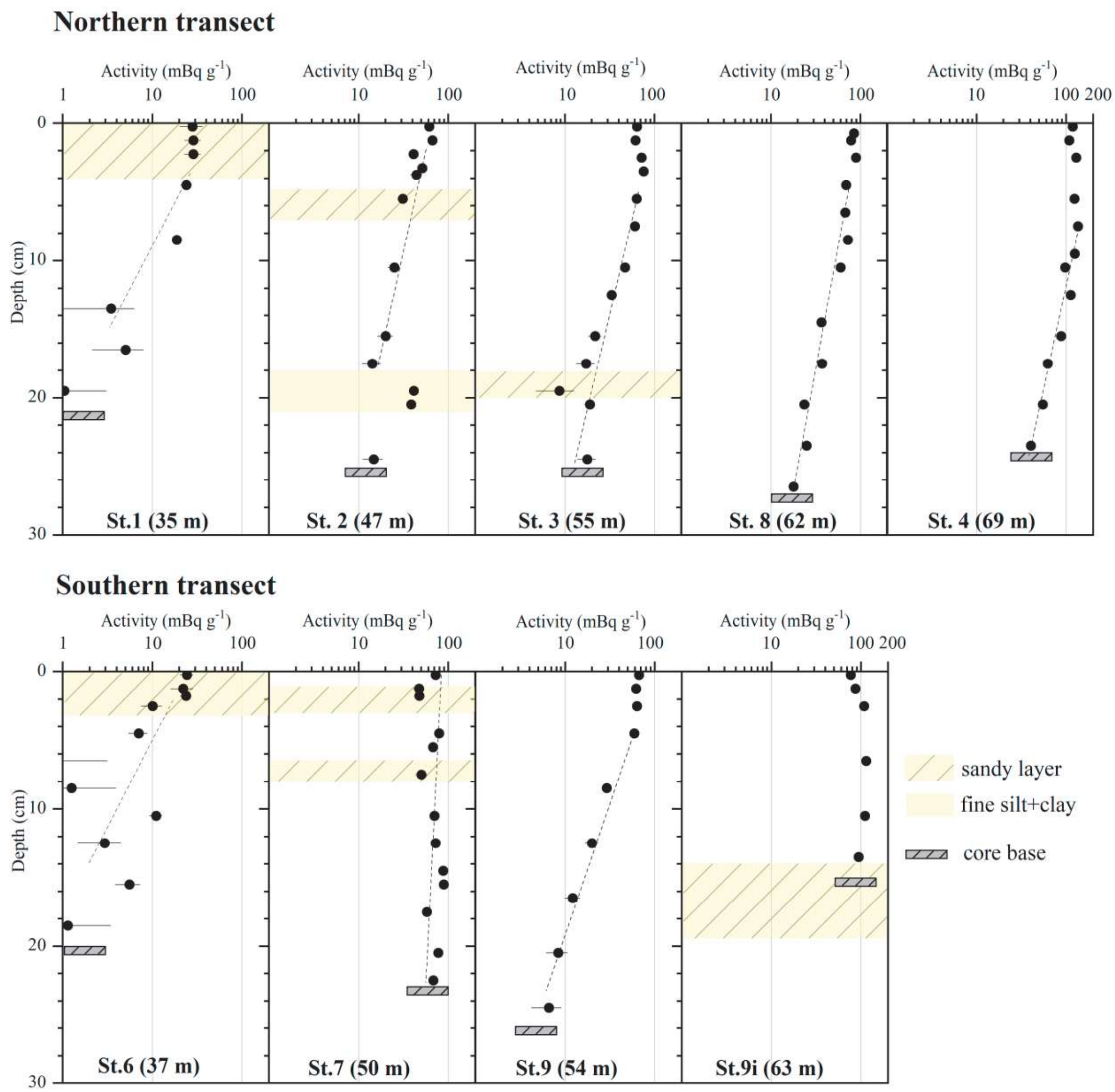

Figure 3: Depth profiles of $^{210}Pb_{xs}$ activity for all the sediment cores collected in the West Gironde Mud Patch in fall 2016. Next to the core label, numbers are the water depth at which the cores were collected. Errors bars correspond to 1 SD. The grey rectangle indicates the length of the core.

Table 1: Mean bottom OC contents, sediment (SAR) and mass (MAR) accumulation rates calculated from $^{210}Pb_{xs}$ profiles and calculated OC burial rates at nine sites of the West Gironde Mud Patch. For stations 1, 6 and 9, the bottom OC values were taken at the base of modern sediments (see Figure 4)

Transect	Stations	Lat.	Long.	Depth	Bottom OC	*n* =	SAR	MAR	OC burial rates
		°N	°E	m	%		cm yr^{-1}	mg cm^{-2} yr^{-1}	gC m^{-2} yr^{-1}
North	1	45°45'38"	- 1°31'41"	35	0.64 ± 0.03*	1	0.14 ± 0.08**	126 ± 73**	8 ± 5**
	2	45°43'45"	- 1°37'57"	47	0.66 ± 0.20	5	0.48 ± 0.09**	486 ± 89**	32 ± 16
	3	45°40'58"	- 1°41'30"	55	0.99 ± 0.12	5	0.38 ± 0.04	361 ± 35	36 ± 8
	8	45°38'55"	- 1°45'48"	62	1.02 ± 0.02	5	0.47 ± 0.05	438 ± 47	45 ± 6
	4	45°36'50"	- 1°49'47"	69	1.30 ± 0.04	4	0.41 ± 0.07	338 ± 56	44 ± 9
South	6	45°44'22"	- 1°30'2"	37	0.42 ± 0.27	2	0.22 ± 0.13**	172 ± 102**	7 ± 9**
	7	45°37'17"	- 1°37'34"	50	1.41 ± 0.19	6	0.97 ± 0.20***	648 ± 122***	-
	9	45°35'54"	- 1°40'9"	54	1.17 ± 0.10	3	0.29 ± 0.03	237 ± 22	28 ± 5
	9i	45°31'25"	- 1°45'20"	63	-	-	2.83***	1413***	-

*analytical incertitude
** apparent maximum SAR, MAR and OC burial rates, presence of sandy layers
*** indicative maximum SAR and MAR - not suitable for calculations

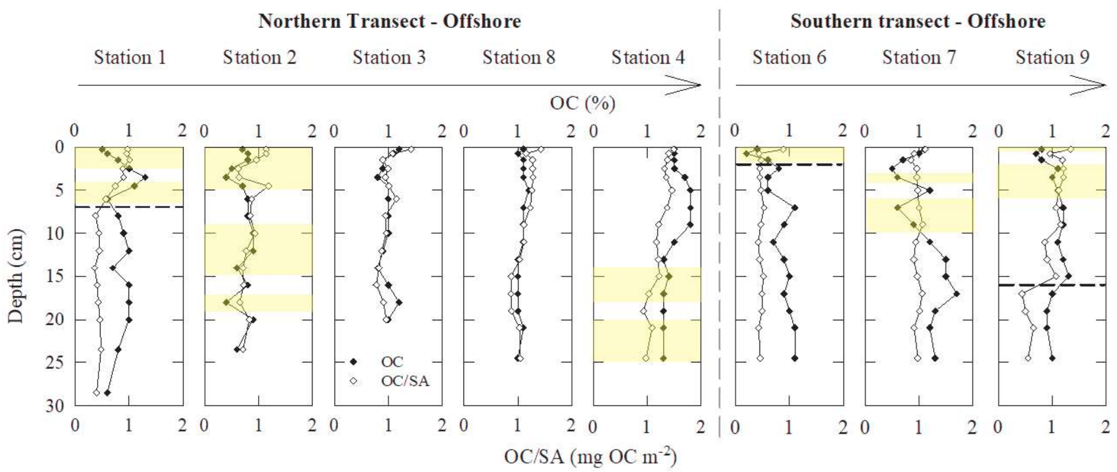

Figure 4: Vertical distributions of OC content (%) and OC/SA ratio (mgOC m^{-2}) in sediment cores collected in the West Gironde Mud Patch. The yellow stripes indicate the position of noticeable sandy layers. Dashed lines represent the limit between modern and relic deposits.

Table 2: Surface and bottom core OC contents (%) and OC/SA ratio (mgOC m^{-2}). *For stations 1, 6 and 9 the bottom values were taken at the base of modern sediments.

Stations (Depth)		OC content (%)		OC/SA (mgOC m^{-2})	
		Surface	Bottom	Surface	Bottom
North	1 (35m)	0.48	0.64*	0.97	0.57*
	2 (47m)	0.70	0.56	1.14	0.71
	3 (55m)	1.15	1.02	1.42	0.96
	8 (62m)	1.08	1.01	1.43	1.04
	4 (69m)	1.53	1.25	1.49	0.98
South	6 (37m)	0.36	0.61*	0.89	0.48*
	7 (50m)	1.09	1.32	1.12	0.98
	9 (54m)	0.84	1.25*	1.34	1.07*

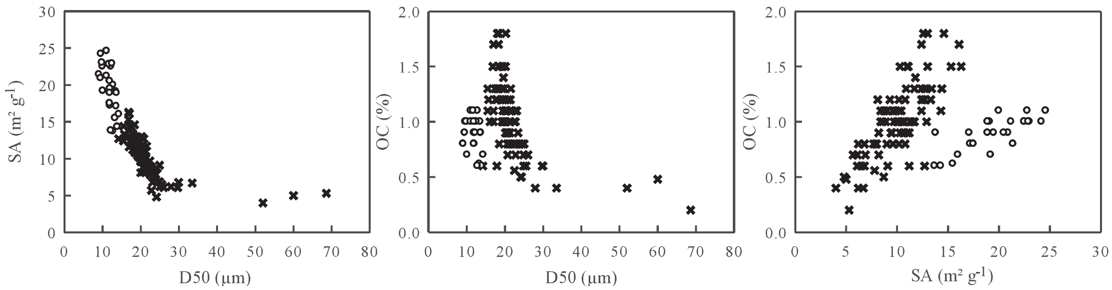

Figure 5: SA against median grain-size (a), sediment OC content against median grain-size (b) and SA (c). Cross correspond to all the sediment samples, excluding the relic sediments (white circles; stations 1, 6 and 9).

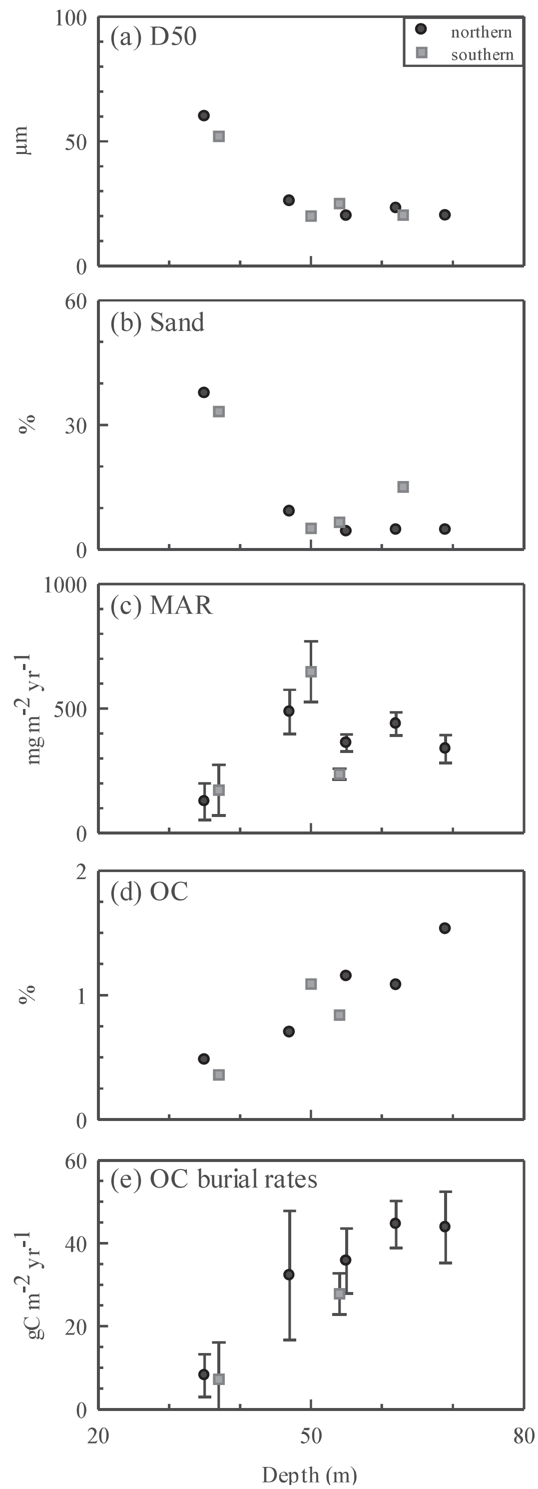

Figure 6: Median grain-size (a), sand (b) and organic carbon (d) content of surface sediments, mass accumulation rates (c) and OC burial rates at multi-decennial scales (e) against water depth of stations along the northern and the southern transects of the West Gironde Mud Patch.

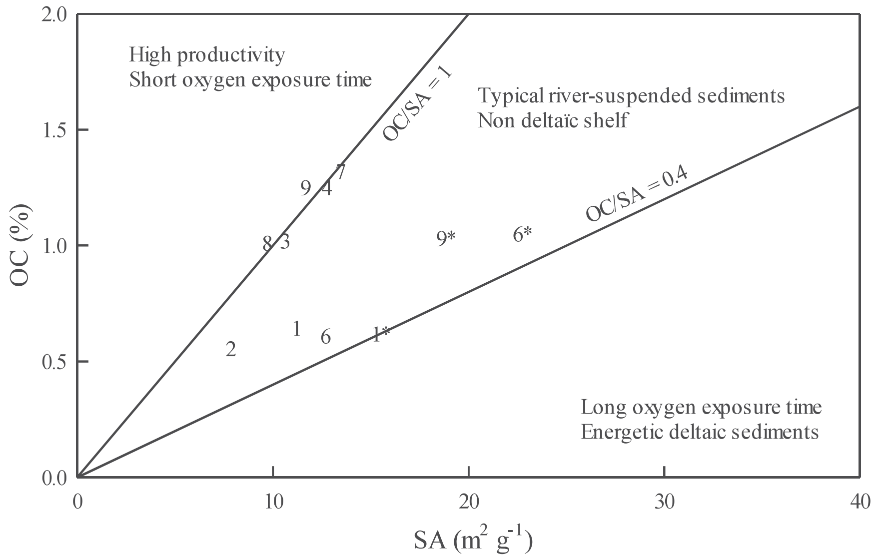

Figure 7: Relationship of OC contents (%) against surface areas of sediments (SA; $m^2 g^{-1}$) at the base of modern and relic (*) sediments of the West Gironde Mud Patch. Adapted from Blair and Aller (2012).

Table 3: Mass accumulation rates and OC burial rates in sediments of (1) the West Gironde Mud Patch (this study) (2) the Bay of Biscay (Mouret et al., 2010), (3) the Goban Spur (Celtic margin, Van Weering et al., 1998), (4) the Iberian Margin (Van Weering et al., 2002), (5) the Gulf of Lions shelf (Accornero et al., 2003) and of (6) the Amazon deltaic shelf (Aller et al., 1996; Kuehl et al., 1986), the Bohai and Yellow Seas (Hu et al., 2016), the Zhejiang-Fujian Mud Zone (East China Sea, Sun et al., 2020), the inner Louisiana shelf (Gordon et al., 2001). The most proximal sites of the WGMP (i.e., 1 and 6) are not considered. *Average values of organic carbon burial rates.

Location	Depth (m)	MAR (mg cm^{-2} yr^{-1})	OC burial rates (gC m^{-2} yr^{-1})	References
WGMP (Bay of Biscay)	47 - 69	237 - 486	28 - 45	This study
Bay of Biscay	550	78	7.32	
Bay of Biscay	1000	36	2.52	
Bay of Biscay	1250	44	2.4	Mouret et al. (2010)
Bay of Biscay	1500	7	0.45	
Bay of Biscay	2000	14	0.96	
Goban Spur	208	<5.8	> 0.16	Van Weering et al. (1998)
Iberian Margin	104	204.2	34.30	
Iberian Margin	123	208.9	9.00	
Iberian Margin	199	150.1	7.09	Van Weering et al. (2002)
Iberian Margin	223	157.1	5.02	
Iberian Margin	343	63.4	3.77	
Gulf of Lions	87	230	19.0	Accornero et al. (2003)
Amazon deltaic shelf	9 - 53	100 - 6900	58.3*	Aller et al. (1996), Kuehl et al. (1986)
Bohai and Yellow Seas	0 - 400	< 100 - 7000	15.3*	Hu et al. (2016)
East China Sea	45.4	200 - 700	41.2*	Sun et al. (2020)
Louisiana shelf	4 - 23	120 - 450	22.7*	Gordon et al. (2001)

Declaration of interests

☒ The authors declare that they have no known competing financial interests or personal relationships that could have appeared to influence the work reported in this paper.

☐The authors declare the following financial interests/personal relationships which may be considered as potential competing interests: